Journal of Controlled Release 164 (2012) 291–298

Contents lists available at SciVerse ScienceDirect

Journal of Controlled Release

journal homepage: www.elsevier.com/locate/jconrel

Nanofibrillar cellulose hydrogel promotes three-dimensional liver cell culture

Madhushree Bhattacharya [a,b,1], Melina M. Malinen [a,b,1], Patrick Lauren [a], Yan-Ru Lou [a], Saara W. Kuisma [a], Liisa Kanninen [a], Martina Lille [c], Anne Corlu [d], Christiane GuGuen-Guillouzo [d], Olli Ikkala [e], Antti Laukkanen [f], Arto Urtti [b], Marjo Yliperttula [a,*]

[a] Division of Biopharmaceutics and Pharmacokinetics, Faculty of Pharmacy, P.O. Box 56, FI-00014 University of Helsinki, Finland
[b] Centre for Drug Research, Faculty of Pharmacy, P.O. Box 56, FI-00014 University of Helsinki, Finland
[c] VTT Technical Research Centre of Finland, P.O. Box 1000, FI-02044 VTT, Finland
[d] Inserm UMR991, Liver Metabolism and cancer, Université de Rennes 1, F-35043 Rennes, France
[e] Department of Applied Physics, Molecular Materials, Aalto University/Helsinki University of Technology, P.O. Box 5100, FI-00076 Aalto, Espoo, Finland
[f] UPM-Kymmene Corporation, Tekniikantie 2C, FI-02150 Espoo, Finland

ARTICLE INFO

Article history:
Received 16 April 2012
Accepted 30 June 2012
Available online 7 July 2012

Keywords:
3D cell culture
Hepatocyte
Nanocellulose
Nanofiber
Plant-derived cellulose

ABSTRACT

Over the recent years, various materials have been introduced as potential 3D cell culture scaffolds. These include protein extracts, peptide amphiphiles, and synthetic polymers. Hydrogel scaffolds without human or animal borne components or added bioactive components are preferred from the immunological point of view. Here we demonstrate that native nanofibrillar cellulose (NFC) hydrogels derived from the abundant plant sources provide the desired functionalities. We show 1) rheological properties that allow formation of a 3D scaffold in-situ after facile injection, 2) cellular biocompatibility without added growth factors, 3) cellular polarization, and 4) differentiation of human hepatic cell lines HepaRG and HepG2. At high shear stress, the aqueous NFC has small viscosity that supports injectability, whereas at low shear stress conditions the material is converted to an elastic gel. Due to the inherent biocompatibility without any additives, we conclude that NFC generates a feasible and sustained microenvironment for 3D cell culture for potential applications, such as drug and chemical testing, tissue engineering, and cell therapy.

1. Introduction

Three dimensional (3D) cell cultures are emerging tools in cell biology, regenerative medicine, cell therapy, chemical testing and drug discovery. Compared to two-dimensional (2D) cultures, the three-dimensional cell cultures mimic more closely the in-vivo tissue. An optimal 3D culturing environment resembles the physiological microenvironment and extracellular matrix (ECM). In tissues the ECM plays a pivotal role in determining the phenotype of cells [1–3]. Mostly, the ECM is composed of glycosaminoglycans and fibrous proteins, such as collagen, elastin, laminin and fibronectin, which are self-assembled into a nanofibrillar network [4,5]. This network provides structural support to the cells and allows biochemical signaling for cellular guidance. It is obvious that cell behavior is highly regulated by the complex interplay of factors that act in 3D microenvironment.

Mostly cell culture experiments are carried out in 2D format using conditions that may be quite different from the real physiological situations. Taken the environmental factors in cell growth and differentiation, the differences of cell culture conditions may lead to erroneous conclusions in the experiments. Therefore, there is a continuing need for improved cell culture systems that would result in proper cellular phenotype, and more reliable cell based research in many fields of biomedicine [6–8].

Artificial ECM mimicking 3D matrices have emerged as a potential strategy towards more realistic *in vivo* like cell culture systems. The 3D matrices (i.e. cell culture scaffolds), are based on natural and/or synthetic biomaterials. Biomaterials provide mechanical support and host relevant biochemical cues (peptides, peptide amphiphiles, carbohydrates, growth factors) to cell growth and differentiation. An ideal matrix for 3D cell growth should mimic the ultrastructure and mechanical properties of native ECM, support cell growth and maintenance with biochemical signals, and yield a framework for transfer of nutrients, waste metabolites and intercellular chemical signaling. In essence, the scaffold should lead to cellular functions that are identical to the native state of the particular cell type. Such optimized cell culture systems have enormous potential in basic biomedical research, drug development, and cell-based transplantations. Predictive cell models for preclinical drug discovery are needed to improve the current success rate of 10% in clinical drug testing [9]. Improved 3D cell culture systems are also needed for tissue engineering and cell transplantation purposes [7]. Finally, recent advances in human stem cell biology (e.g. induced pluripotent stem cells) underline the need for 3D cell culture systems that would support proper 3D phenotype of the cells during differentiation process [10].

* Corresponding author. Tel.: +358 440 935566; fax: +358 9 191 59580.
E-mail address: marjo.yliperttula@helsinki.fi (M. Yliperttula).
[1] These authors contributed equally to this work.

0168-3659 © 2012 Elsevier B.V. Open access under CC BY-NC-ND license.
doi:10.1016/j.jconrel.2012.06.039

Hydrogels are promising class of materials for 3D cell culture [11–18]. In hydrogels, a network of interconnected pores enables retention of high water content, and efficient transport of oxygen, nutrients and waste products [12]. Hydrogels from both synthetic and natural sources have been used for 3D cell culture. The bioactive components of hydrogels can be defined (e.g. peptide-based materials such as PuraMatrix™ or peptide amphiphiles) or undefined (extracts from animal or human origin, like Matrigel™, MaxGel™). Undefined biomaterials are well suited for 3D cell culture *in vitro*, but they cannot be used for *in vivo* cell therapy and tissue engineering.

Various kinds of polysaccharides molecularly dissolved in aqueous media have been used scaffolds for tissue engineering, but typically they require separate cross-linking step to form the hydrogel network [19]. By contrast, the native cellulose nanofibers produced in bacteria and plants [16] form colloidal level dispersions in aqueous medium instead of solubility. They have mechanically strong native crystalline structure, lateral dimensions in the nanometer length scale and they can have high aspect ratio leading to aqueous gels [20], encouraging for cell culturing experiments. The bacterial cellulose scaffolds have already proven to be suitable for the tissue engineering of hard tissues like bone and cartilage [16,21]. Plant derived native nanofibrillar cellulose has not found application in tissue engineering. Native plant derived nanofibers can be isolated from plant cell walls using intensive mechanical shearing combined with chemical and enzymatic pre-treatments or TEMPO oxidation [20,22,23]. Therein, aligned β-D-glucopyranose polysaccharide chains form mechanically strong cellulose I crystals with hydrogen bonded parallel polymer chains. In aqueous environment, these native cellulose nanofibers form hydrogels even at low concentrations, typically down to 0.1–0.2 wt.% [20].

This study demonstrates the feasibility of plant derived native nanofibrillar cellulose (NFC) hydrogels as 3D-cell culture scaffolds. The material is interesting due to its defined single component structure, tunability of hydrogel properties, and availability. Structural properties of NFC hydrogel were investigated, and their properties as cell culture scaffolds were evaluated using hepatocyte and retinal pigment epithelial cell lines. We show that a single component NFC scaffold promotes hepatocyte 3D cell culture without added bioactive components. To the best of our knowledge this is the first report using plant derived NFC for 3D soft tissue culture.

2. Materials and methods

2.1. Biomaterials

Nanofibrillar cellulose (NFC) hydrogel was obtained from UPM-Kymmene Corporation, Finland. The nanofibers were isolated from bleached birch pulp via a controlled homogenization process using an industrial fluidizer. The raw material was aseptically collected from a UPM pulp mill and thoroughly purified prior to homogenization with sterilized machinery. Thus, the microbial purity was maintained through the whole production process. Purified pulp fibers were diluted with sterilized, ultra high quality water before the fibrillation. The NFC concentration of the resulting hydrogel is typically 1.7 wt.%. Prior to cell culturing the NFC hydrogels were autoclaved (121 °C 20 min). For reference, the commercial cell culturing hydrogels; MaxGel™ (MG), ExtraCel™ (EC), HydroMatrix™ (HM), PuraMatrix™ peptide (PM) were purchased from Sigma–Aldrich, Glycosan biosystems, Sigma–Aldrich, BD Biosciences, respectively.

2.2. Electron microscopy

Scanning electron microscopy images were acquired using a JEOL JSM-7500FA Field-Emission SEM. The diameter of fibrils was measured from SEM images using image analysis software as described earlier [22]. Cryo-transmission electron microscopy was carried out using a dedicated field emission cryo-electron microscope (JEOL JEM-3200FSC) operated at 300 kV. The method is described in more detail elsewhere [22].

2.3. Rheological measurements

Rheological measurements of the NFC hydrogel were carried out at room temperature with a stress controlled rotational rheometer (AR-G2, TA instruments, UK) equipped with four-bladed vane geometry. The diameters of the cylindrical sample cup and the vane were 30 mm and 28 mm, respectively. The length of the vane was 42 mm. The viscoelastic properties of the hydrogel were determined with a frequency sweep and a time sweep in dynamic oscillatory mode of the rheometer at a strain of 0.1 wt.%. The steady state viscosity was measured in the shear stress range of 0.01–100 Pa.

2.4. Injectability of nanofibrillar cellulose hydrogel cell culture

The hydrogel culture was initiated by mixing ARPE-19 cells with 1.7 wt.% NFC at a density of 25,000 cells per 200 μl in a 96 well plate. Cells were cultured for 48 h prior the injection with a 1 ml syringe and different sized needles (20 G–27 G) into a new 96-well plate. After the transfer the cells were cultured further 24 h and the viability was assayed using resazurin (see cell viability paragraph) and a spectral scanning plate reader (Varioskan®, Thermo Scientific).

2.5. Optical properties of nanofibrillar cellulose hydrogel

Absorbance and fluorescence were recorded to determine the optical properties of NFC hydrogel. UV–vis absorbance of 0.5 wt.% NFC was recorded in the 300–550 nm range with a UV spectrometer (QuantaMaster™, Photon Technology International) using cuvette of path length 1 mm. The fluorescence spectra from different concentrations of the hydrogel were measured with a spectral scanning plate reader after exciting at 405, 488 and 560 nm. The excitation wavelengths were selected to reflect usual biological imaging. We used 10 μg/ml Hoechst 33258, 6 μg/ml FITC-dextran 70 kDa and 10 mM rhodamine 123 as the positive controls for each excitation wavelength. Purified water was the negative control.

2.6. Diffusion studies

Diffusion studies were performed to model the transport of nutrients to the cells and the mobility of incorporated macromolecules through NFC hydrogel. The hydrogels were loaded with different FITC-dextran probes (20, 70, and 250 kDa molecular weight). Stock solutions and further dilutions of FITC-dextran probes were prepared in PBS buffer at a final concentration of 125 μg/ml. Briefly in a transwell system 200 μl of FITC/dextran was added to the apical chamber containing 300 μl of hydrogel. Samples were taken from the lower (basolateral) chamber periodically to quantify the fluorescence intensity in the lower chamber. The first eight samples were taken at 15 min intervals; there after samples were withdrawn at 30 min intervals for 4 h. Samples taken from the recipient compartment were replaced with buffer. The permeability of the NFC correlates with the fluorescence intensity. Fluorescence was measured using a spectral scanning plate reader (ex490, em530). All diffusion experiments were done at 25 °C.

2.7. Cell cultures

Hepatic progenitor HepaRG cells were obtained from a liver tumor of a female patient suffering from hepato-cholangiocarcinoma [24] and were cultured as described previously [24]. Human hepatocellular carcinoma HepG2 cells (ATCC HB-8065) were cultured in high glucose Dulbecco's modified Eagle's medium supplemented with 10% fetal bovine serum, 100 U/ml penicillin, 100 μg/ml streptomycin,

2 mM L-glutamine and 100 mM sodium pyruvate. Human ARPE-19 cells (ATCC CRL-2302) were cultured in DMEM-F12 (1:1) supplemented with 10% fetal bovine serum, 2 mM L-glutamine, 100 U/ml penicillin and 100 μg/ml streptomycin. For all cell lines the medium was renewed every 2 or 3 days. For cell viability and growth studies, the cells were seeded at a density of 5×10^4 cells/cm^2 (0% hydrogel), or at 2.5×10^4 cells/cm^2 (corresponding to 1000 cells/μl of biomaterial in 3D). For albumin secretion analysis, HepG2 cells were seeded in different hydrogels at a density of 2.6×10^5/cm^2 (corresponding to 1053 cells/μl of biomaterial) and HepaRG cells were seeded at a density of 13×10^4 cells/cm^2 (corresponding to 500 cells/μl of biomaterial). The following biomaterials were used for cell encapsulation: MaxGel™ ECM (MG), Extracel™ hydrogel (EC), 0.25% HydroMatrix™ peptide cell culture scaffold (HM), 0.25% PuraMatrix™ peptide hydrogel (PM), and 0.1–1.2 wt.% novel NFC hydrogel. The hydrogel formation and encapsulation of cells in MG, EC, HM and PM were performed according to the manufacturer´s instructions (Sigma–Aldrich, Glycosan biosystems, Sigma–Aldrich, BD Biosciences, respectively). After gelation medium was added to each hydrogel culture. 3D NFC cell culture was prepared by mixing the cell suspension with NFC to achieve 0.1–1.2 wt.% hydrogels, after which the medium was added. HepaRG were cultured for 30 days and HepG2 cells for 5 days, respectively.

2.8. Cell viability

The mitochondrial metabolic activity of the cells was accomplished by the addition of oxidation–reduction indicator, resazurin (alamarBlue® Cell Viability Reagent), 1/10 of medium volume. After 4 h exposure to resazurin at 37 °C in 5% CO_2, 100 μl of medium was transferred from each well to a 96 well plate and the fluorescent metabolite of resazurin (resorufin) was recorded with a spectral scanning plate reader (ex560 and em590). Additionally cell viability was analyzed by introducing 10 μM fluorescein diacetate (FDA) in serum-free medium. The conversion of non-fluorescent FDA into fluorescent fluorescein was followed with Leica TCS SP5 II HCS A confocal microscope at 37 °C and 5% CO_2.

2.9. Total protein analysis

Cells were lysed with RIPA buffer with protease inhibitor cocktail according to the manufacturer's procedures (Pierce Biotechnology, USA). Protocols for monolayer-cultured cells and suspension-cultured cells were followed for standard and 3D cultures, respectively. Total protein of cell culture lysates was quantified with BCA Protein Assay Kit (Pierce Biotechnology, USA).

2.10. Albumin secretion

To investigate the liver-specific functions of hydrogel embedded cells, the **s**ecreted albumin levels were determined with Human Albumin ELISA kit according to the manufacturer´s instructions (Bethyl Laboratories, USA). Each collected medium sample was measured in duplicates and diluted (1:2–1:100) to fit into kit´s standard curve.

2.11. F-actin staining and confocal imaging

The structure of spheroids was analyzed by fixing the cell cultures in 3% paraformaldehyde for 15 min. After washing with PBS, the cells were permeabilized with 0.1% Triton X-100 for 15 min and subsequently incubated overnight with Alexa Fluor 594-labeled phalloidin (Invitrogen A12381, diluted 1:100 or 1:50 in PBS) to visualize cellular distribution of the filamentous actin cytoskeleton. The nuclei were stained with 1 μg/ml Hoechst 33258. Labeled samples were protected with an antifade reagent (Prolong gold, Invitrogen) and analyzed with a confocal microscope (either Leica TCS SP5 or Leica TCS SP2 AOBS). The confocal images were analysed with Imaris 7.4 program (Bitplane) and either slice or surpass images were constructed. The possible deconvolution was done with AutoQuant X program (MediumCybernetics).

3. Results and discussion

3.1. Electron microscopy studies

Cryo-TEM image of vitrified NFC hydrogel (Fig. 1A) shows that the diameter of the smallest individual cellulose nanofiber is close to 7 nm and that the majority of the material forms larger bundled structures. Analysis from SEM images showed that the most common fibril width was between 20 and 30 nm due to some aggregation (Fig. 1B). The exact length of the nanofibers cannot be estimated from the images due to the entangled and bundled nature of the material. It seems however that the individual nanofibers are several micrometers in length. We point out that the dimensions of the cellulose nanofibers revealed by images resemble those of native collagen. [25]

3.2. Rheological properties

In aqueous environment, dispersion of cellulose nanofibers formed a viscoelastic hydrogel network. The gel was formed at relatively low concentrations by dispersed and hydrated entangled fibrils. The viscoelasticity of the NFC hydrogel were characterized with dynamic oscillatory rheological measurements. The frequency sweep in Fig. 2A shows typical behavior of a NFC hydrogel [26], where the storage modulus (G') is much higher than the loss modulus (G'') and nearly independent of frequency (Fig. 2A).

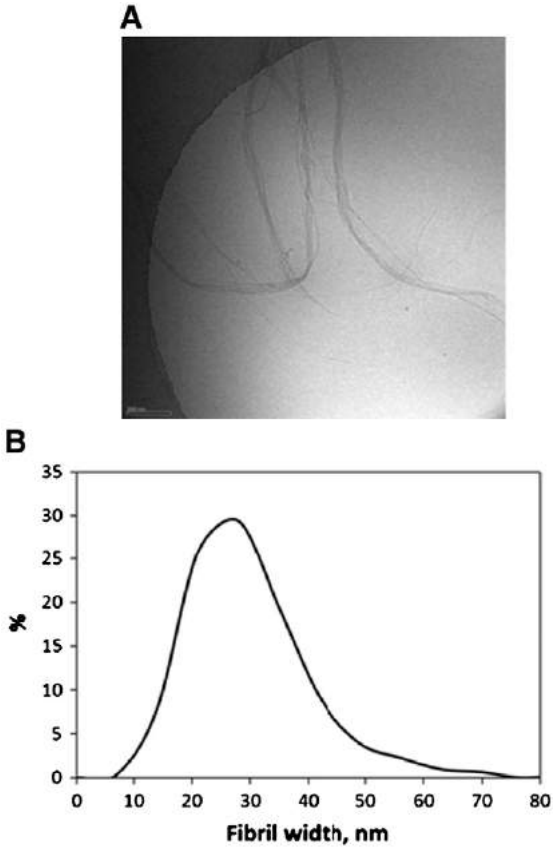

Fig. 1. (A) Cryo-TEM image of vitrified NFC hydrogel. The scale bar, 200 nm. (B) Fibril width distribution measured manually from FE-SEM image.

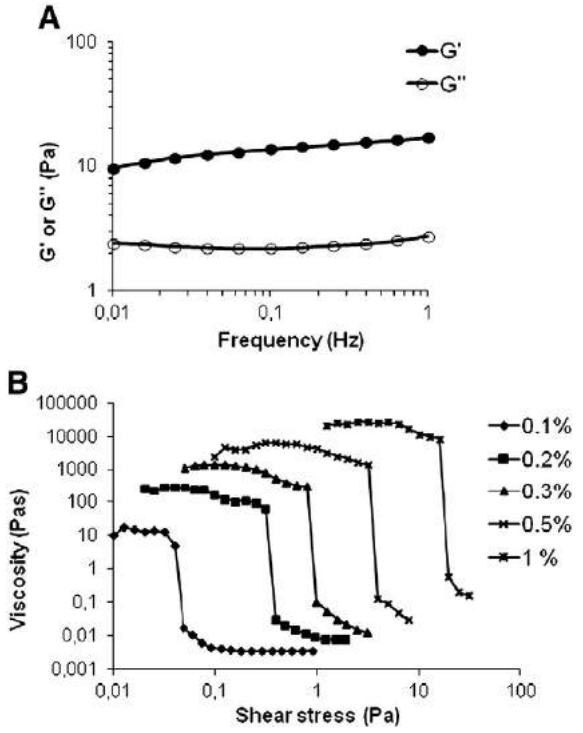

Fig. 2. Rheological properties of nanofibrillar cellulose hydrogel. (A) Frequency dependence of storage (G') and loss modulus (G'') of a 0.5wt.% hydrogel. (B) Flow curves of 0.1–1 wt.% hydrogel as function of shear stress.

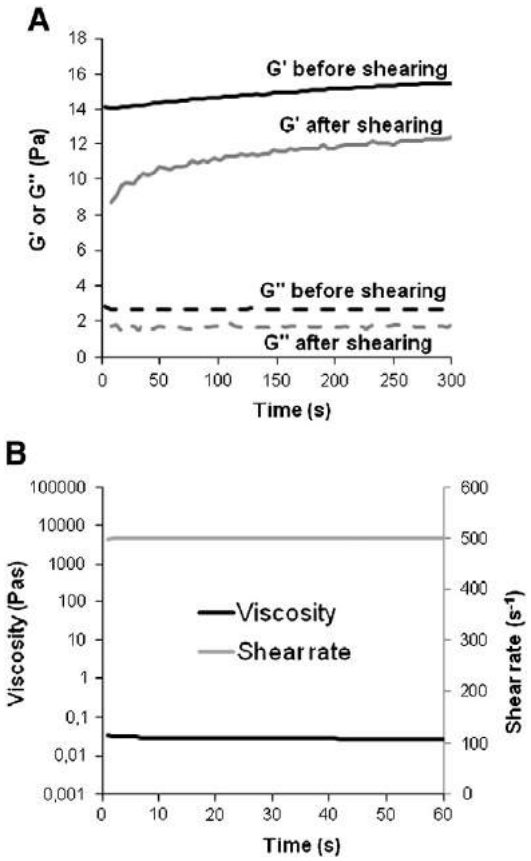

Fig. 3. (A) Structure of 0.5 wt.% nanofibrillar cellulose hydrogel recovers after high-speed (500 s^{-1}) shearing. (B) Evolution of viscosity when a 0.5 wt.% NFC gel was sheared at a constant shear rate of 500 s^{-1}.

Importantly, the rheology of the NFC hydrogels show reversible gelation, see Fig. 2B: Using a stress controlled rheometer, at high stress levels (valid for injections) a fluid-like behavior is observed whereas at low stress level and quiescent conditions a step-wise transition to solid-like behavior is observed below at critical stress level. The viscoelastic properties of the NFC hydrogels are similar to those of physiological ECMs [25].

Changes in temperature have only a minor effect on the viscoelastic properties of NFC hydrogels. Thus, the situation is quite different compared to other cellulose based hydrogels formed *e.g.* by methyl cellulose that shows lower critical solution temperature at 40–50 °C. This difference arises mainly from the inherent structure of fibrils compared to macromolecular structure of soluble cellulose derivates. In NFC hydrogels, majority of the macromolecules are aligned in the crystalline domain of the nanofiber structure. Therefore, a change in the environment does not trigger conformational changes of the polymer chains, which means that the gel strength is almost constant over very broad temperature, pH, or ionic strength range. On the other hand, with soluble cellulose derivates, like methyl cellulose, increase in temperature causes the polymer chain to contract due to increased hydrophobic attraction, which eventually leads to macroscopic changes of the whole aqueous system.

The perceived 10 Pa G' is an encouraging finding considering cell culturing application, because collagen matrices exhibiting $G' \approx 4$–60 Pa have shown to support 3D soft tissue culture (human fibroblasts) [25]. At rest (at low levels of shear stress) the NFC network exhibits very high viscosity at low concentrations (Fig. 2B). This property is necessary to keep the cells in 3D environment, as a suspension in the gel. Application of a certain critical shear stress results in a dramatic decrease in the hydrogel viscosity (Fig. 2B) presumably due to the disruption of the gel network. This kind of shear-thinning behavior of the NFC hydrogel is beneficial, since it allows mixing of cells into the gel and easy dispensing of the hydrogel cell cultures, e.g. with a syringe and needle, a pipette tip, or a microfluidic device. An additional important rheological property of NFC hydrogels is that the high viscosity is established instantaneously after shearing (e.g. injection or mixing) has stopped. This was demonstrated by shearing the gel for 1 min at 500 s^{-1} in the rheometer

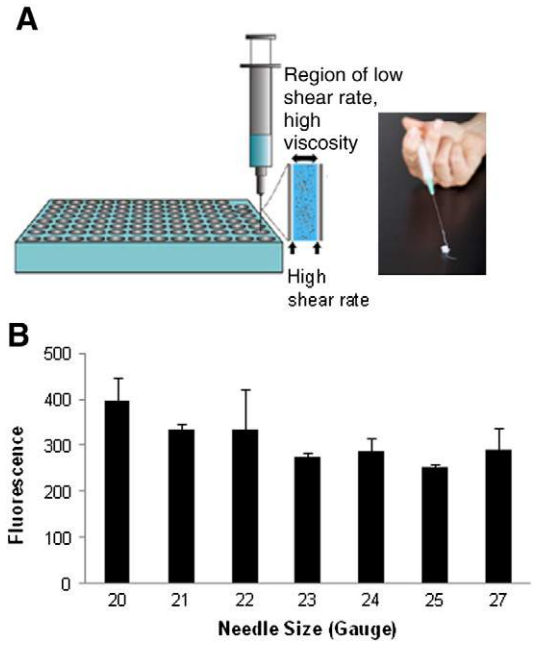

Fig. 4. Injectability of nanofibrillar cellulose hydrogel cell culture. (A) Schematic drawing depicting regions of low and high shear rates in the needle during injection of NFC hydrogel cell culture. (B) Cells remained viable after the injection with syringe needles of different sizes. Fluorescence from the viability marker resorufin is shown on the Y axis.

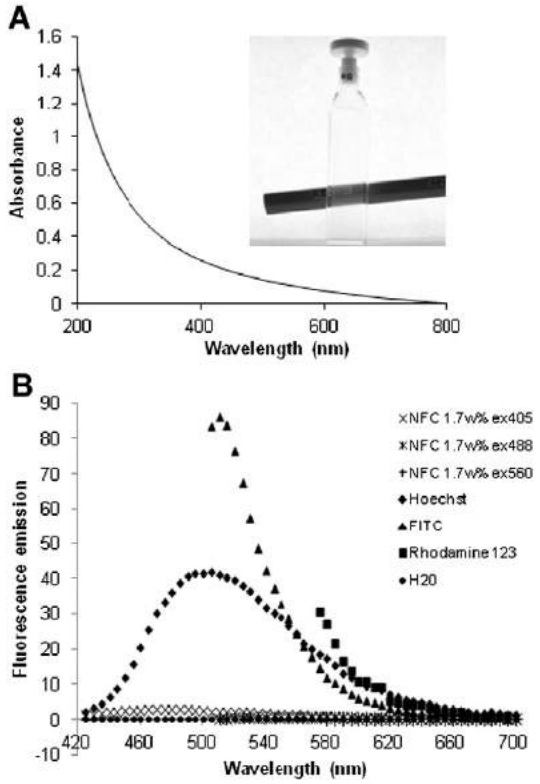

Fig. 5. (A) Absorbance spectrum of 0.5 wt.% NFC hydrogel at the UV–visible wavelengths. The inset image visualizes the transparency of the hydrogel in the measurement cuvette. (B) Fluorescence spectra of hydrogels compared to purified water at excitation wavelengths of commonly used molecular probes (405, 488 and 560 nm).

(Fig. 3B) and by following the evolution of the viscoelastic properties of the material (at rest) immediately after shearing period. Viscoelastic gel network ($G' >> G''$) was restored within a few seconds (Fig. 3A).

Obviously, the mechanical properties of 0.1–1 wt.% NFC hydrogels are different than in the bacterial cellulose scaffolds [16,21,27]. For example, the Young's modulus of microporous bacterial cellulose scaffold is 1.58 MPa, which was considered well suitable for bone regeneration [27].

3.3. Injectability of nanofibrillar cellulose hydrogel cell culture

The effect of dispensing conditions on cell viability was studied by transferring NFC cell culture with a syringe and needles of different sizes (Fig. 4). NFC hydrogel with cells may be transferred even with the smallest needle (27 G) without affecting cell viability (Fig. 4B). The cells were not damaged by the injection related shear stress. The shear-thinning property of the hydrogel may aid in keeping cells viable as it reduces the volume of suspension subjected to very high shear rates (Figs. 4A, 2B). A 20 G size needle is equivalent to a 1–300 μl pipette tip routinely used in dispensing of cell suspensions.

3.4. Optical properties

Although the cellulose nanofibers are very thin, they scatter some light due to their association into fiber bundles with a thickness larger than 50 nm. NFC hydrogels (0.01–1 wt.%) do not absorb light at UV and visible wavelengths (Fig. 5A). The high absorbance peak seen close to 200 nm corresponds to light scattering (Fig. 5A). No autofluorescence originate from the NFC (Fig. 5B). Thus though, optical detection of NFC hydrogel with light microscopy may be limited due to light scattering. Lack of autofluorescence allows fluorescence spectroscopy based imaging with low background unlike with other biomaterial scaffolds [28].

3.5. Diffusion in nanofibrillar cellulose hydrogel

To model the nutrient supply to the cells within the 3D NFC hydrogels, the permeability of FITC-dextrans (20–250 kDa) was investigated. Permeability studies showed transfer of the FITC-dextrans in NFC hydrogels (Fig. 6A, B). Permeability coefficient of FITC-dextran increased from 10^{-7} to 10^{-6} cm/s with decreasing mean molecular weight of the permeating compound. Assuming hydrogel thickness of 3 mm and hydrogel/water partition coefficient (K) of 1.0 (i.e. no binding or exclusion of the FITC-dextrans from the hydrogel), the diffusion coefficients (D) FITC-dextrans in NFC hydrogel range from 3×10^{-8} to 10^{-7} cm^2/s. These values are approximately equal with those of proteins in the natural extracellular matrices suggesting adequate diffusivity of nutrient, hormones and other essential compounds in NFC hydrogel [29].

3.6. Biocompatibility characterization

HepaRG and HepG2 cell culture experiments on various concentrations of the hydrogel assayed biocompatibility of the NFC. NFC hydrogel was not cytotoxic for HepaRG and HepG2 cells at concentrations of 0.1–1 wt.% (Fig. 6E–H). This agrees with previously published reports of fibrillated cellulose [16]. Cell viability in hydrogel culture did not differ from the conventional cell cultures. Additionally, fluorescein diacetate labeling showed that both cell types were viable and formed 3D spheroids within the hydrogel (Fig. 6G, H).

NFC embedded HepaRG and HepG2 cells exhibited non-exponential growth based on the total protein assay, while classical exponential growth was observed on the standard cell cultures (Fig. 6C, D). In hydrogel, the amount of HepG2 cells doubled in eight days (Fig. 6D), whereas HepaRG cells showed less proliferation (Fig. 6C). The slower growth in NFC hydrogel is in agreement with previous findings with hydrogel-encapsulated cells [30–34] and is related to mechanical stimuli from the NFC hydrogel. It has been recognized that physical parameters are important determinants of cell growth and phenotype regulation [35].

3.7. Three-dimensional cell culture of HepG2 and HepaRG

Finally, we investigated the potential of native NFC hydrogel, without additional bioactive ECM components, in supporting the cellular differentiation of the human hepatic cell lines, HepG2 and HepaRG. Both HepG2 and HepaRG formed 3D multicellular spheroids in NFC hydrogel, such a trend was also seen in hyaluronan-gelatin-polyethylene glycol diacrylate hydrogel (Extracel™, EC), and in peptide nanofiber hydrogels (HydroMatrix™, HM and PuraMatrix™, PM) (Fig. 7A, data not shown). Previously HepG2 multicellular aggregate formation has been demonstrated in poly(N-isopropylacrylamide) hydrogel [36], on chitosan film [37] and in bioreactors [38]. HepaRG spheroid formation has not been shown earlier.

The filamentous actin staining shows accumulation at the site of apical membranes in HepaRG spheroids (Fig. 7B). Enhanced formation of F-actin between apical cells assert the in vivo-like polarity and are known to be associated with bile canaliculus formation [39]. HepG2 spheroids however were not as clearly polarized even though they were regular in shape (Fig. 7B). Both PM and NFC supported cell spheroid formation (Fig. 7B). Differentiation state of the cell spheroids was further studied using albumin secretion as biomarker (Fig. 7C, D). The results suggest that the cells do secrete albumin in the NFC hydrogel supported cultures. It is good to notice that all the other cell cultures were in 3D, but Maxgel™ (MG) supports only 2D cell culture, and was thus used as 2D reference for 3D cell cultures. HepaRG progenitor cells increased the secretion during four weeks

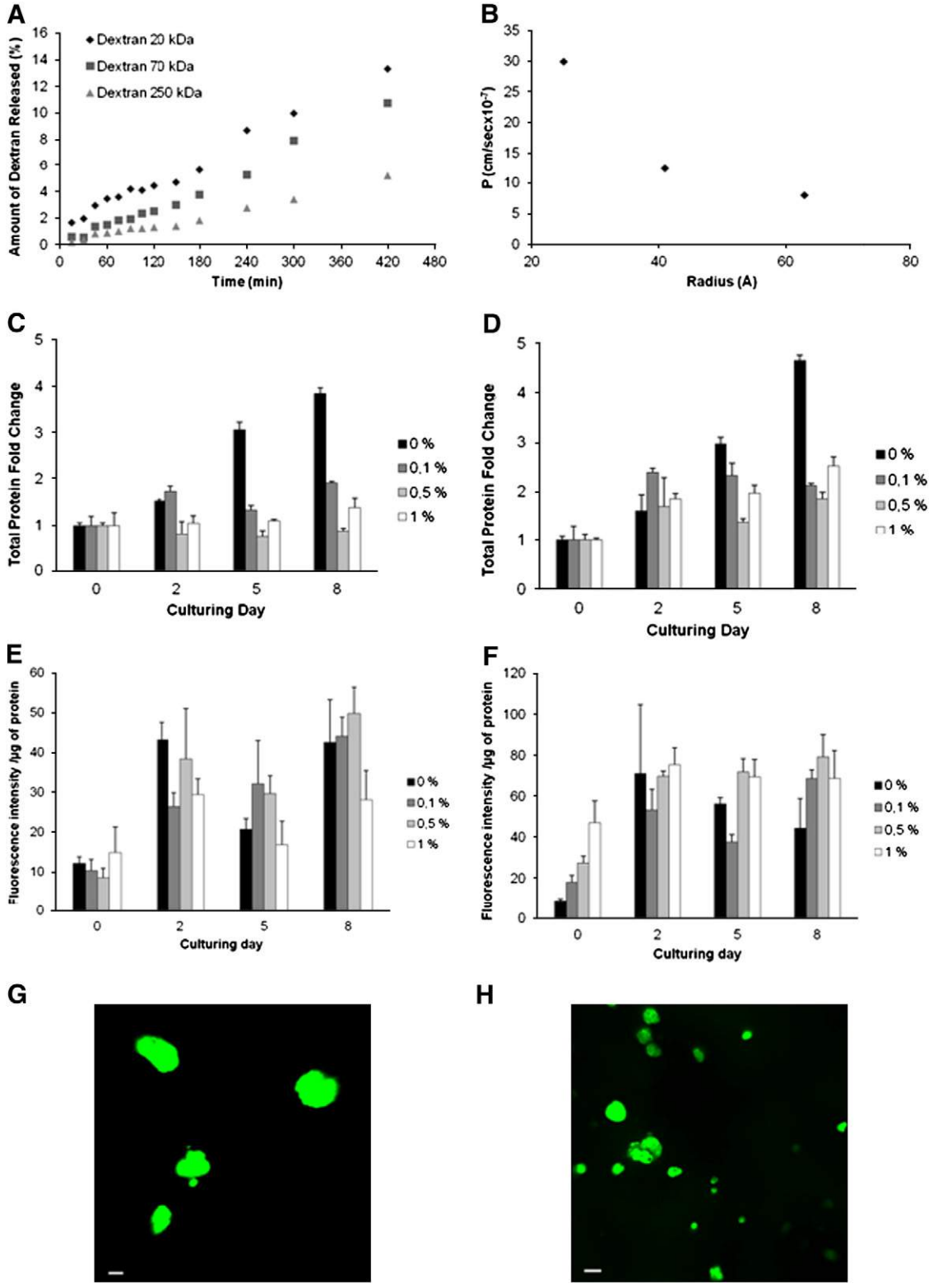

Fig. 6. Permeability and biocompatibility properties of NFC hydrogels. (A) Release of fluorescently labeled dextrans (FITC-dextrans) from 0.5 wt.% hydrogel. (B) Relationship between molecular radius of FITC-dextrans and their permeability (P) in hydrogel. (C, E) HepaRG and (D, F) HepG2 cells were cultured at various concentrations of NFC hydrogel (wt.%) and without hydrogel (0 wt.%). (C, D) The growth and (E, F) viability of the cells were analyzed. The viability of (E) HepaRG and (F) HepG2 cells were comparable between NFC hydrogel and standard cultures. Viability was maintained during the whole culture time. Viability of 30 days HepaRG culture and 4 days HepG2 culture in the 0.7 wt.% hydrogel was studied using fluorescein diacetate (FDA). After 10 min incubation, the viable (G) HepaRG and (H) HepG2 spheroids converted FDA into fluorescent fluorescein (green). The scale bars are (G) 20 µm, and (H) 50 µm.

of culture implicating the process of differentiation (Fig. 7C). Previously, HepaRG progenitor cells have been found to undergo morphological and functional differentiation process on standard cell culture environment [40,41], on fibronectin coated 3D micropatterns [42] and in bioreactor [43]. Differentiation was most evident in NFC and EC scaffolds where secretion increased 4–8 folds from the initiation

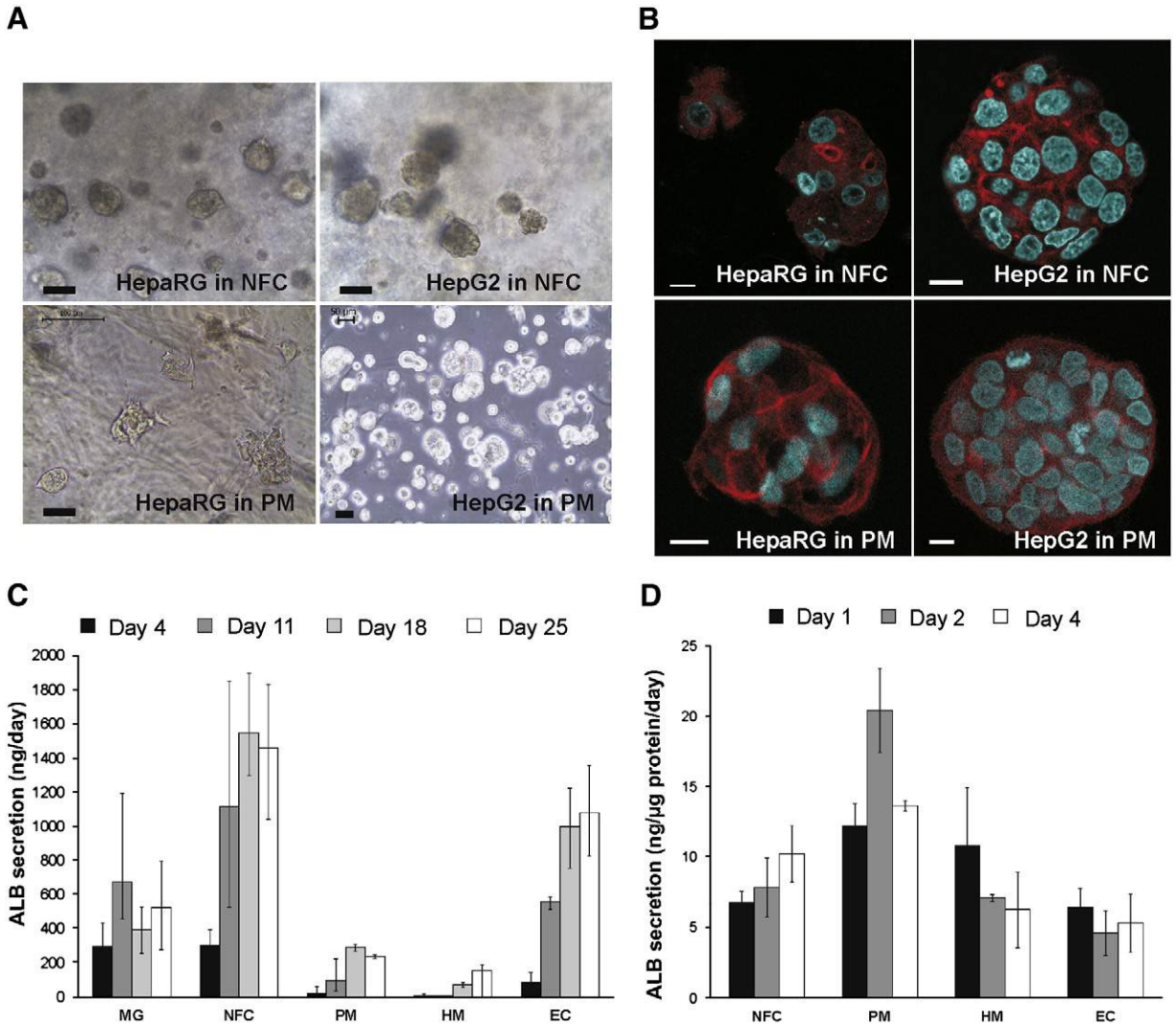

Fig. 7. Morphology and albumin secretion of HepaRG and HepG2 cells in diverse hydrogel cultures. Cells formed spheroids in nanofibrillar cellulose (NFC) and in peptide nanofiber (Puramatrix™, PM) hydrogel cultures, as evidenced by (A) phase contrast microscopy, and (B) confocal microscopy with structural staining of filamentous actin (red) and nuclei (blue). (C) Albumin secretion of HepaRG evolved during the 25 days of culture (D) while secretion from HepG2 remained stable during the 4 days culture. HepaRG in NFC after (A) 8 days and (B) 15 days, and in PM after (A) 6 days and (B) 30 days of culture. HepG2 in NFC after (A) 6 days and (B) 4 days, and in PM after (A) 5 days and (B) 7 days of culture. The scale bars are (A) 50 μm, and (B) 10 μm. Maxgel™ (MG), Extracel™ (EC), Hydromatrix™ (HM), Puramatrix™ (PM), and nanofibrillar cellulose (NFC). (C) Error bars represent mean ± min-max values for n = 2–4. (D) Error bars represent mean ± standard deviations for n = 3.

of cultures. The levels of secreted albumin from HepG2 cells embedded in NFC matched with the biomaterials that provide biochemical cues (PM, HM, EC) (Fig. 7D). The results clearly show that a non-human and non-animal derived single component NFC hydrogel is able to support 3D growth and differentiation of liver cells.

4. Conclusions

Herein, we report plant-derived native nanofibrillar cellulose hydrogel as a cell culture scaffold. NFC hydrogel constructed 3D environment for the cells and induced spheroid formation of HepaRG and HepG2 cells. No cytotoxicity was observed and mitochondrial activity was equal in standard 2D and nanofibrillar cellulose cultures. The viscoelastic properties of plant derived NFC hydrogel scaffold differ considerably from previously studied bacterial cellulose scaffolds. NFC was found to be injectable due to fluid-like behavior at high stress due to reversible gelation and rheological characteristics allowed mixing of cells into the gel. The spontaneously formed gel state after injection provided the required mechanical support for cell growth and differentiation. Beneficial properties of NFC are based on its unique nanofibrillar structure mimicking properties of the ECM.

Acknowledgments

This work was funded and supported by the Tekes-The Finnish Funding Agency for Technology and Innovation, EU-FP7 (LIV-ES project, HEALTH-F5-2008-223317), Graduate School of Pharmaceutical Sciences and Academy of Finland (grant 118650).

Covadonga Parras-Cicuendez from the Complutence University of Madrid (EU-Erasmus Exchange Student Exchange Programme), National Nanomicroscopy Center (Panu Hiekkataipale and Janne Ruokolainen) from Aalto University, Finland, and Unto Tapper from VTT Technical Research Centre of Finland, are gratefully acknowledged for assisting in cell viability studies, taking cryo-TEM and field emission SEM images, respectively.

References

[1] H.K. Kleinman, M.L. McGarvey, J.R. Hassell, V.L. Star, F.B. Cannon, G.W. Laurie, G.R. Martin, Basement membrane complexes with biological activity, Biochemistry 25 (1986) 312–318.

[2] S.L. Bowers, I. Banerjee, T.A. Baudino, The extracellular matrix: at the center of it all, J. Mol. Cell. Cardiol. 48 (2010) 474–482.

[3] R.C. Dutta, A.K. Dutta, Cell-interactive 3D-scaffold; advances and applications, Biotechnol. Adv. 27 (2009) 334–339.

[4] H. Fernandes, L. Moroni, C. van Blitterswijk, J. de Boer, Extracellular matrix and tissue engineering applications, J. Mater. Chem. 19 (2009) 5474–5484.

[5] H.K. Kleinman, M.L. McGarvey, L.A. Liotta, P.G. Robey, K. Tryggvason, G.R. Martin, Isolation and characterization of type IV procollagen, laminin, and heparan sulfate proteoglycan from the EHS sarcoma, Biochemistry 21 (1982) 6188–6193.

[6] D.J. Maltman, S.A. Przyborski, Developments in three-dimensional cell culture technology aimed at improving the accuracy of in vitro analyses, Biochem. Soc. Trans. 38 (2010) 1072–1075.

[7] F. Gelain, A. Horii, S.G. Zhang, Designer self-assembling peptide scaffolds for 3-D tissue cell cultures and regenerative medicine, Macromol. Biosci. 7 (2007) 544–551.

[8] F. Pampaloni, E.G. Reynaud, E.H.K. Stelzer, The third dimension bridges the gap between cell culture and live tissue, Nat. Rev. Mol. Cell Biol. 8 (2007) 839–845.

[9] U.S. Food and Drug Administration, Report - Challenge and Opportunity on the Critical Path to New Medical Products in, 2004.

[10] A.W. Lund, B. Yener, J.P. Stegemann, G.E. Plopper, The natural and engineered 3D microenvironment as a regulatory cue during stem cell fate determination, Tissue Eng. Part B Rev. 15 (2009) 371–380.

[11] C. Wang, R.R. Varshney, D.A. Wang, Therapeutic cell delivery and fate control in hydrogels and hydrogel hybrids, Adv. Drug Delivery Rev. 62 (2010) 699–710.

[12] J.L. Drury, D.J. Mooney, Hydrogels for tissue engineering: scaffold design variables and applications, Biomaterials 24 (2003) 4337–4351.

[13] M.W. Tibbitt, K.S. Anseth, Hydrogels as extracellular matrix mimics for 3D cell culture, Biotechnol. Bioeng. 103 (2009) 655–663.

[14] S.G. Zhang, T.C. Holmes, C.M. Dipersio, R.O. Hynes, X. Su, A. Rich, Self-complementary oligopeptide matrices support mammalian-cell attachment, Biomaterials 16 (1995) 1385–1393.

[15] J.P. Miranda, A. Rodrigues, R.M. Tostoes, S. Leite, H. Zimmerman, M.J. Carrondo, P.M. Alves, Extending hepatocyte functionality for drug-testing applications using high-viscosity alginate-encapsulated three-dimensional cultures in bioreactors, Tissue Eng. C Meth. 16 (2010) 1223–1232.

[16] D. Klemm, F. Kramer, S. Moritz, T. Lindstrom, M. Ankerfors, D. Gray, A. Dorris, Nanocelluloses: a new family of nature-based materials, Angew. Chem. Int. Ed Engl. 50 (2011) 5438–5466.

[17] J.B. Matson, S.I. Stupp, Self-assembling peptide scaffolds for regenerative medicine, Chem. Commun. 48 (2012) 26–33.

[18] S.M. Zhang, M.A. Greenfield, A. Mata, L.C. Palmer, R. Bitton, J.R. Mantei, C. Aparicio, M.O. de la Cruz, S.I. Stupp, A self-assembly pathway to aligned monodomain gels, Nat. Mater. 9 (2010) 594–601.

[19] Y. Cheng, X. Luo, G.F. Payne, G.W. Rubloff, Biofabrication: programmable assembly of polysaccharide hydrogels in microfluidics as biocompatible scaffolds, J. Mater. Chem. 22 (2012) 7659–7666.

[20] M. Paakko, M. Ankerfors, H. Kosonen, A. Nykanen, S. Ahola, M. Osterberg, J. Ruokolainen, J. Laine, P.T. Larsson, O. Ikkala, T. Lindstrom, Enzymatic hydrolysis combined with mechanical shearing and high-pressure homogenization for nanoscale cellulose fibrils and strong gels, Biomacromolecules 8 (2007) 1934–1941.

[21] J. Andersson, H. Stenhamre, H. Backdahl, P. Gatenholm, Behavior of human chondrocytes in engineered porous bacterial cellulose scaffolds, J. Biomed. Mater. Res. A 94A (2010) 1124–1132.

[22] J. Vartiainen, T. Pohler, K. Sirola, L. Pylkkanen, H. Alenius, J. Hokkinen, U. Tapper, P. Lahtinen, A. Kapanen, K. Putkisto, P. Hiekkataipale, P. Eronen, J. Ruokolainen, A. Laukkanen, Health and environmental safety aspects of friction grinding and spray drying of microfibrillated cellulose, Cellulose 18 (2011) 775–786.

[23] T. Saito, S. Kimura, Y. Nishiyama, A. Isogai, Cellulose nanofibers prepared by TEMPO-mediated oxidation of native cellulose, Biomacromolecules 8 (2007) 2485–2491.

[24] P. Gripon, S. Rumin, S. Urban, J. Le Seyec, D. Glaise, I. Cannie, C. Guyomard, J. Lucas, C. Trepo, C. Guguen-Guillouzo, Infection of a human hepatoma cell line by hepatitis B virus, Proc. Natl. Acad. Sci. U. S. A. 99 (2002) 15655–15660.

[25] M. Miron-Mendoza, J. Seemann, F. Grinnell, The differential regulation of cell motile activity through matrix stiffness and porosity in three dimensional collagen matrices, Biomaterials 31 (2010) 6425–6435.

[26] A.H. Clark, S.B. Rossmurphy, Structural and mechanical-properties of bio-polymer gels, Adv. Polym. Sci. 83 (1987) 57–192.

[27] M. Zaborowska, A. Bodin, H. Backdahl, J. Popp, A. Goldstein, P. Gatenholm, Microporous bacterial cellulose as a potential scaffold for bone regeneration, Acta Biomater. 6 (2010) 2540–2547.

[28] I.H. Jaafar, C.E. LeBlon, M.T. Wei, D. Ou-Yang, J.P. Coulter, S.S. Jedlicka, Improving fluorescence imaging of biological cells on biomedical polymers, Acta Biomater. 7 (2011) 1588–1598.

[29] S.R. Chary, R.K. Jain, Direct measurement of interstitial convection and diffusion of albumin in normal and neoplastic tissues by fluorescence photobleaching, Proc. Natl. Acad. Sci. U. S. A. 86 (1989) 5385–5389.

[30] C.E. Semino, J.R. Merok, G.G. Crane, G. Panagiotakos, S. Zhang, Functional differentiation of hepatocyte-like spheroid structures from putative liver progenitor cells in three-dimensional peptide scaffolds, Differentiation 71 (2003) 262–270.

[31] J.S. Park, D.G. Woo, B.K. Sun, H.M. Chung, S.J. Im, Y.M. Choi, K. Park, K.M. Huh, K.H. Park, In vitro and in vivo test of PEG/PCL-based hydrogel scaffold for cell delivery application, J. Control. Release 124 (2007) 51–59.

[32] Y. Lei, S. Gojgini, J. Lam, T. Segura, The spreading, migration and proliferation of mouse mesenchymal stem cells cultured inside hyaluronic acid hydrogels, Biomaterials 32 (2011) 39–47.

[33] T.P. Kraehenbuehl, P. Zammaretti, A.J. Van der Vlies, R.G. Schoenmakers, M.P. Lutolf, M.E. Jaconi, J.A. Hubbell, Three-dimensional extracellular matrix-directed cardioprogenitor differentiation: systematic modulation of a synthetic cell-responsive PEG-hydrogel, Biomaterials 29 (2008) 2757–2766.

[34] L.S. Wang, J. Boulaire, P.P.Y. Chan, J.E. Chung, M. Kurisawa, The role of stiffness of gelatin-hydroxyphenylpropionic acid hydrogels formed by enzyme-mediated crosslinking on the differentiation of human mesenchymal stem cell, Biomaterials 31 (2010) 8608–8616.

[35] F. Brandl, F. Sommer, A. Goepferich, Rational design of hydrogels for tissue engineering: impact of physical factors on cell behavior, Biomaterials 28 (2007) 134–146.

[36] D. Wang, D. Cheng, Y. Guan, Y. Zhang, Thermoreversible hydrogel for in situ generation and release of HepG2 spheroids, Biomacromolecules 12 (2011) 578–584.

[37] P. Verma, V. Verma, P. Ray, A.R. Ray, Formation and characterization of three dimensional human hepatocyte cell line spheroids on chitosan matrix for in vitro tissue engineering applications, in vitro cellular & developmental biology, Animal 43 (2007) 328–337.

[38] T.T. Chang, M. Hughes-Fulford, Monolayer and spheroid culture of human liver hepatocellular carcinoma cell line cells demonstrate distinct global gene expression patterns and functional phenotypes, Tissue Eng. Part A 15 (2009) 559–567.

[39] R. Sormunen, S. Eskelinen, V.P. Lehto, Bile canaliculus formation in cultured Hepg2 cells, Lab. Invest. 68 (1993) 652–662.

[40] C. Aninat, A. Piton, D. Glaise, T. Le Charpentier, S. Langouet, F. Morel, C. Guguen-Guillouzo, A. Guillouzo, Expression of cytochromes P450, conjugating enzymes and nuclear receptors in human hepatoma HepaRG cells, Drug Metab. Dispos. 34 (2006) 75–83.

[41] V. Cerec, D. Glaise, D. Garnier, S. Morosan, B. Turlin, B. Drenou, P. Gripon, D. Kremsdorf, C. Guguen-Guillouzo, A. Corlu, Transdifferentiation of hepatocyte-like cells from the human hepatoma HepaRG cell line through bipotent progenitor, Hepatology 45 (2007) 957–967.

[42] E. Mercey, P. Obeid, D. Glaise, M.L. Calvo-Munoz, C. Guguen-Guillouzo, B. Fouque, The application of 3D micropatterning of agarose substrate for cell culture and in situ comet assays, Biomaterials 31 (2010) 3156–3165.

[43] M. Darnell, T. Schreiter, K. Zeilinger, T. Urbaniak, T. Soderdahl, I. Rossberg, B. Dillner, A.L. Berg, J.C. Gerlach, T.B. Andersson, Cytochrome P450-dependent metabolism in HepaRG cells cultured in a dynamic three-dimensional bioreactor, Drug Metab. Dispos. 39 (2011) 1131–1138.